Chinese Chemical Letters 34 (2023) 108101

Contents lists available at ScienceDirect

Chinese Chemical Letters

journal homepage: www.elsevier.com/locate/cclet

Induction heating enables efficient heterogeneous catalytic reactions over superparamagnetic nanocatalysts

Chao Huang[a], Yu Wang[b], Rui Zhong[b], Zhenkun Sun[a,*], Yonghui Deng[c,*], Lunbo Duan[a,*]

[a] Key Laboratory of Energy Thermal Conversion and Control of Ministry of Education, School of Energy and Environment, Southeast University, Nanjing 210096, China
[b] Key Laboratory of Functional Molecular Solids, Ministry of Education, Anhui Key Laboratory of Molecule-Based Materials, College of Chemistry and Materials Science, Anhui Normal University, Wuhu 241002, China
[c] Department of Chemistry, State Key Laboratory of Molecular Engineering of Polymers, Fudan University, Shanghai 200433, China

ARTICLE INFO

Article history:
Received 30 November 2022
Revised 12 December 2022
Accepted 23 December 2022
Available online 29 December 2022

Keywords:
Induction heating
Magnetic particles
Cross-coupling reaction
Heterogeneous catalysis
Core-shell

ABSTRACT

Most catalytic processes are achieved by heating the whole reaction systems including the entire reactor, substrate and solvent, which leads to energy loss and obvious heat transfer limits. In this study, induction heating was employed to boost the catalytic Suzuki-Miyaura cross-coupling reactions by using conductive superparamagnetic microspheres with loaded Pd nanoparticles as heterogeneous catalysts. It was found that, at the same apparent reaction temperatures, the reactions by adopting the induction heating all exhibit better catalytic performance with higher conversion and yield, as compared to the reactions using conventional joule heating. The improvement is mainly attributed to the localized heating effect endowed by high efficiency of the heat transfer from the heat source to catalytic sites, which dissipates the electromagnetic energy through Néel relaxation mechanism. Moreover, it has be found that the reactions have been largely accelerated, resulting in much shorter reaction time required to approach a given value of reactant conversion. These results indicate that the unique heating method based on the superparamagnetic nanomaterials as both the inductive component and catalyst support holds a promising application for fast and efficient heterogeneous catalytic process, and exhibits potential for improving energy transfer efficiency and reducing the side reactions attributed to the uneven temperature profile.

Catalysis is a crucial route to improve process efficiency for chemical and material production in various industry sectors. Several factors, such as by-products formation, energy efficiency, reactor optimization, and cost-effectiveness, have long been considered momentous restrictions during the development of the traditional catalytic processes [1–4]. In the last decades, advances in catalysis were mainly achieved through the development of high activity multifunctional catalysts, as well as innovative process design. For the latter, improving the heat and mass transfer in the catalytic process is one of the most strategic ways. The conventional heating method such as the joule heating (JH) for catalysis usually heats the overall reactor based on heat conduction, convection and radiation such as the situation in a tube furnace for gas-solid reactions. Such heating scheme always results in an obvious temperature gradient from the heat source to the solid catalysts and further to the surface active sites, accompanied by a considerable energy loss and potential by-products generation [5]. Recently, new schemes including microwave heating [6,7], laser heating [8,9] and plasma technology [10], have been reported to improve the heat transfer process so as to reduce adverse effects in heating the catalytic reactions.

Induction heating (IH) recently has become a unique heating scheme for catalysis, in which the heat generates directly from the inductive materials, usually the solid catalysts, and is immediately transferred outward to reactants and reaction media. Such a contactless heating method exhibits significant advantages in maintaining heterogeneous catalytic reactions. On one hand, the heat generates almost instantaneously from the electrically conductive or magnetic catalysts due to the selective absorption of radiofrequency energy, which significantly reduces thermal inertia and improves the uniformity of temperature distribution in the reaction media. On the other hand, the IH provides only the energy of heat that is necessary to induce the catalytic reaction on the active sites of catalysts, thus avoiding heating the whole reactor/reaction media and minimizing considerably the heat loss and energy input. During the induction heating, the heat generated under the high-

* Corresponding authors.
E-mail addresses: zhenkun_sun@seu.edu.cn (Z. Sun), yhdeng@fudan.edu.cn (Y. Deng), duanlunbo@seu.edu.cn (L. Duan).

https://doi.org/10.1016/j.cclet.2022.108101
1001-8417/

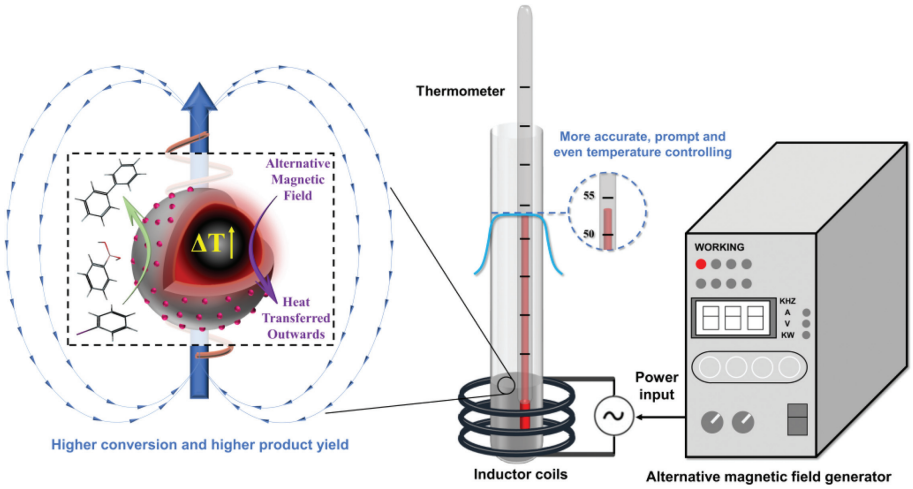

Fig. 1. Schematic for the catalytic cross-coupling reaction sustained by induction heating under alternative magnetic fields leading to a more accurate and even temperature control over the nanocatalyst and reaction media.

frequency alternating magnetic fields (AMF) mainly follows three mechanisms: eddy currents, hysteresis or relaxation losses induced in metals and ferromagnetic materials [11–13]. Several pioneering study on the use of induction heating for catalysis have been done by the Kirschning's group [14–16]. They have employed the magnetic nanoparticles loaded with specific active sites as an inductively heatable catalyst to support a series of liquid-solid catalytic reactions under continuous-flow conditions. Henceforth, various inductive catalysts with enhanced magnetic properties, optimized curie temperature and improved specific absorption rate have been designed and applied also for gas-solid catalytic reactions such as dry and steam methane reforming [17–21], Fischer-Tropsch syntheses [22], methanation reactions [23–27], volatile organic compounds (VOCs) degradation [28,29].

The liquid-solid catalytic reactions are usually conducted under batch-by-batch reaction mode, thus the whole reactor in conventional catalytic process has to be heated. The direction of energy transmission during heating is generally from the external energy generator to the liquid phase, then to the catalyst. In fact, the catalyst surface temperature is lower than the temperature of the solvent and reactor container, especially for endothermic reactions. When the catalyst surface reaches the critical temperature that can trigger the target catalytic reaction, the temperature of the whole container or the solvent will be higher, which may lead to negative effects such as the degradation of reactants, acceleration of by-products generation and also the waste of heat. While, the introduction of the IH can reversely switch the energy transmission direction in conventional catalytic process, which is anticipated to provide a higher temperature on the catalyst surface but keep the temperature of reaction media and reactor lower. In such a sense, when maintaining the same catalytic activity of a given reaction, temperature of the overall reaction media or reactor sustained by IH can be kept lower compared to those sustained by conventional external heating. In this study, we have conducted a comprehensive investigation on the effectiveness of the IH in lower the temperature of reaction media and improving the reaction performance of liquid-solid reactions, when compared to the conventional JH. As shown in Fig. 1, the well-known Suzuki-Miyaura cross-coupling reaction has been selected as a probe liquid-solid catalytic reaction. Meanwhile, the Pd-decorated core-shell structured magnetic microspheres have been adopted as an effective conductive catalyst by virtue of advantages of core-shell structure in combining magnetic material and active sites as a whole.

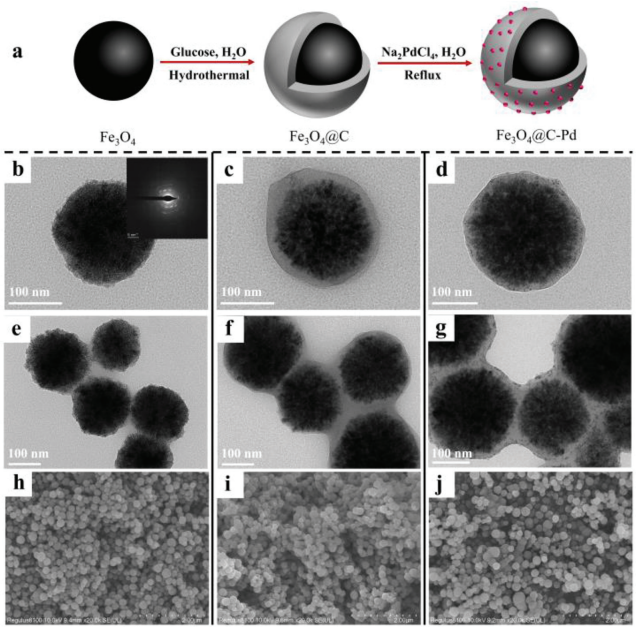

Fig. 2. (a) The synthesis route for Fe_3O_4@C-Pd microspheres. (b–g) TEM and (h-j) SEM images of (b, e and h) magnetic Fe_3O_4 particles, (c, f and i) the Fe_3O_4 particles coated with a carbon layer, and (d, g and j) the obtained catalyst of Fe_3O_4@C-Pd microspheres.

The procedure for synthesizing the catalyst of Pd-decorated magnetic microspheres, designated as Fe_3O_4@C-Pd, can be found in Fig. 2a [30,31]. In particular, the magnetic cores of Fe_3O_4 particles were firstly prepared *via* a robust solvothermal reaction based on a high-temperature reduction of Fe(III) salts with ethylene glycol in the presence of trisodium citrate. Transmission electron microscopy (TEM) images (Figs. 2b and e) show that the synthesized magnetic cores are loose clusters with a nearly uniform size of about ~200 nm. The particles are composed of ultrafine nanocrystals with the size of about ~10 nm estimated from the TEM image. Selected area electron diffraction (SAED) exhibits spotty diffraction rings indicating a polycrystalline-like diffraction and suggests that it consists of many magnetite nanocrystals (Fig. 2b, inset). Scanning electron microscopy (SEM) (Fig. 2h) demonstrates the uniform size and the nearly spherical shape of the magnetic core, which is in good agreement to the TEM results. Then, a uniform

Table 1
Suzuki-Miyaura cross-coupling results of iodobenzene and phenylboronic acid with induction heating (IH) and joule heating (JH) using Fe_3O_4@C-Pd as catalyst.[a]

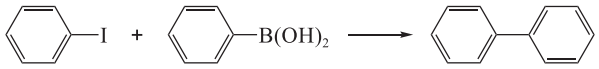

Entry	Temperature (°C)	Catalyst mass (mg)	Reactant equiv.	Conversion (%)[e]		Yield (%)[e]	
				IH	JH	IH	JH
1	38	100	1	28.5	25.5	12.0	10.2
2[b]	54	0	1	–	4.2	–	0
3	54	50	1	52.7	42.3	37.4	29.4
4[c]	54	100 (Fe_3O_4)	1	19.1	11.4	0	0
5	54	100	1	63.5	49.4	38.5	30.7
6	54	200	1	64.0	50.4	48.1	32.5
7[d]	54	200	0.5	69.4	61.9	26.5	25.9
8	54	400	1	71.9	54.5	52.5	40.7
9	72	100	1	100	83.8	80.8	74.3

[a] Reaction conditions: phenylboronic acid (1.5 equiv.), iodobenzene (1 equiv.), TBAB (2 equiv.), Na_2CO_3 (2 equiv.), H_2O (10 mL), reaction time (1 h).
[b] The control entry without using and catalyst is unable to be conducted experiment under IH mode because of no magnetic core.
[c] The control entry using solid without and catalytic Pd nanoparticles.
[d] The dosage of all reactants is reduced to half of the original, but the amount of solvent is still 10 mL.
[e] Conversion of iodobenzene and yield of biphenyl are determined by GC analysis.

carbon layer was coated on the surface of Fe_3O_4 particles through a hydrothermal treatment in the presence of glucose, resulting in core-shell particles denoted as Fe_3O_4@C. TEM observation indicates that a uniform carbonaceous layer of about ~10 nm thickness was formed on individual magnetic cores, leading to a core-shell structure (Figs. 2c and f). In addition, SEM image reveals that the Fe_3O_4@C shows a more regular spherical shape with a smoother surface than the Fe_3O_4 core (Fig. 2i). Finally, Pd nanoparticles were decorated on the surface of Fe_3O_4@C particles through a refluxing treatment of the materials in a water/ethanol solution in the presence of Na_2PdCl_4 as the Pd precursor without using any extra reducing agents. According to the TEM and SEM results, numerous monodispersed Pd nanoparticles are uniformly formed on the carbon shell (Figs. 2d and g), and the obtained Fe_3O_4@C-Pd microspheres show a discrete spherical morphology (Fig. 2j). As shown in Figs. S3a and b (Supporting information), the fine dots pointed out by red arrows on the carbon layer are the Pd NPs. Fig. S3c (Supporting information) shows the high-angle annular dark field (HAADF) images combined with electron dispersive X-ray spectroscopy (EDS) mapping images for Fe_3O_4@C-Pd, which further affirm the successful decoration of the microspheres with Pd NPs. According to the analysis of inductively coupled plasma optical emission spectroscopy (ICP-OES), the contents Fe and Pd in the obtained Fe_3O_4@C-Pd microspheres are 49.0 and 1.20 wt%, respectively. Fig. S4 (Supporting information) exhibits wide angle XRD patterns of the catalyst during each synthesis step. It can be seen that all peaks are corresponding to the Fe_3O_4 phase. The characteristic diffraction peak associated to Pd phase is not observed because of the low Pd content. Fig. S5 (Supporting information) shows the XPS spectrum of the Fe_3O_4@C-Pd catalyst and the corresponding Fe 2p and Pd 3d spectra, which confirms the presence of Pd in the Fe_3O_4@C-Pd catalyst.

The Suzuki-Miyaura cross-coupling reaction involves the reaction between phenylboronic acid and iodobenzene, which is one of the premier routes for the formation of carbon-carbon bonds between aromatics [32]. In this study, the water was selected as solvent due to its environmentally benign and fine dispersive ability provided to the reactants and Fe_3O_4@C-Pd microsphere catalysts. During IH process, the magnetic core in the Fe_3O_4@C-Pd catalyst acts as a susceptor for the conversion of electromagnetic energy into heat. The heat generated in the interior of the Fe_3O_4@C-Pd microspheres can be transferred to the catalytic sites of surface Pd nanoparticles, and subsequently to the aqueous solvent. Three representative reaction media temperatures of 38, 54 and 72 °C have been calibrated under steady-state heat balance and selected for conducting the reaction under IH for sustaining the reaction. For a contrast, the same reaction with using the same reactor at the same temperatures but under JH was conducted in a water bath. The schematic representation of the both processes is presented in Fig. S1 (Supporting information).

All the test entries have been listed in Table 1. Fig. 3 shows the performance of the reaction between iodobenzene and phenylboronic acid catalyzed by the Fe_3O_4@C-Pd microspheres at different temperatures (Figs. 3a and b) under IH or JH by using different amounts of catalyst (Figs. 3c and d). It can be seen from Figs. 3a and b that the reaction supported by IH always exhibits a higher conversion of iodobenzene and yield of biphenyl, when compared to the same reaction supported by JH regardless of reaction temperatures. In particular, the substrate of iodobenzene can be fully converted at 72 °C under IH, while a conversion of only 83% is achieved under JH at the same temperature. Undoubtedly, if the iodobenzene has to be fully converted under the JH, the temperature of reaction media should be higher than 72 °C. This has demonstrated that the IH can effectively lower the temperature of the reaction media. The difference in conversion and yield between using different heating methods of IH and JH is attributed to the difference between the temperature of overall reaction media and that of the catalytically active sites, *i.e.,* Pd nanoparticles. Since the heat is generated on the catalyst core of inductive Fe_3O_4@C particles, the reaction media can only be heated to the setting temperature, such as 54 °C, until enough heat is transferred from the catalyst to the reaction media. In such a way, when the reaction media reach 54 °C, the local temperature on the surface of the Fe_3O_4@C-Pd microsphere should be much higher. Therefore, the active sites of Pd nanoparticles sitting on the surface of Fe_3O_4@C-Pd can catalyze the reaction at a temperature higher than 54 °C at the liquid-solid interface. Differently, during the reaction supported by the JH *via* a water bath, the heat is generated outside the reactor, and the temperature of the Pd nanoparticles on Fe_3O_4@C-Pd microspheres cannot be higher than the overall temperature of the reaction media since the heat should be transferred from the reaction media to the catalyst. As a result, the conversion of iodobenzene is higher under IH than under JH due to the higher local temperature of the Pd active sites during the reaction.

Figs. 3c and d show the conversion of iodobenzene and yield of biphenyl, respectively, during the reaction at 54 °C by using different amounts of catalyst under either IH or JH. It can be seen that the heating method of IH leads to iodobenzene conversions in the

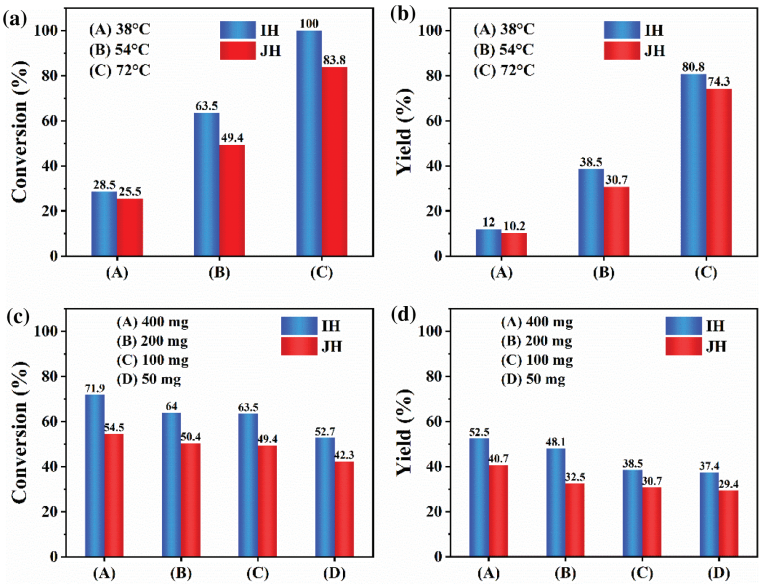

Fig. 3. The catalytic performance of the reaction for 1 h between iodobenzene and phenylboronic acid: (a) The conversion of iodobenzene during the reaction at 38, 54 and 72 °C, supported by IH and JH, respectively, and (b) the corresponding yield of biphenyl. (c) The conversation of iodobenzene and (d) the corresponding yield of biphenyl during the reaction at 54 °C supported by IH and JH, respectively, by using different amounts of catalyst.

range of 52.7%–71.9% and biphenyl yields of 37.4%–52.5%, whereas, iodobenzene conversions of only 42.3%–54.5% and biphenyl yields of 29.4%–40.7% are obtained by using JH (Figs. 3c and d). Meanwhile, the iodobenzene conversion and biphenyl yield all decrease monotonously with the decrease of catalyst mass from 400 mg to 50 mg for both the reactions under IH and JH. However, both the iodobenzene conversion and biphenyl yield are higher in the reaction under IH than that under JH, regardless of catalyst mass. This observation can be attributed to two factors. Firstly, it can be envisaged that reducing the amount of catalyst leads to the decrease of numbers of catalytically active site, which will lower the reactant conversion and product yield under a given reaction conditions. On the contrary, higher catalyst mass will improve the reaction performance in terms of higher conversion and yield. During the reaction under IH, in order to keep the reaction media constant at 54 °C, the temperature on the surface of the Fe_3O_4@C-Pd catalyst should be much higher when using less catalyst since less inductively heatable materials in the reaction media. The higher catalyst surface temperature during the reaction using less catalyst should improve the reactant conversion and product yield compared to the reaction containing catalyst with lower surface temperature. Obviously, the promotion effect of higher catalyst surface temperature over the reaction when using less inductively heatable catalyst is overwhelmed by the negative effect imposed by reducing the number of catalytically active sites. As a result, the conversion and yield both decrease with using less catalyst. Secondly, the carbon middle layer of the Fe_3O_4@C-Pd microsphere catalyst provides a heat shielding effect which narrows the temperature difference between the catalyst surface and the reaction media. As a result, the promotion effect imposed by the temperature difference between catalyst and reaction media is largely weakened in the existence of the carbon middle layer. More recently, Dorman *et al.* have reported a quantitative test on the temperature of Fe_3O_4 and Fe_3O_4@SiO_2 surfaces under IH in liquid media *via* a newly established method of using inorganic luminescent probes. It has been found that the temperature at surface of the Fe_3O_4@SiO_2 can be 64 °C lower than that at surface of uncoated Fe_3O_4 under the same applied AMF [33].

To investigate further, the mass ratio of reactant substrate to solvent has been varied. The experiment has been conducted by using half equivalent substrate with 200 mg catalysts in the same volume of water solvent. The corresponding catalytic performance is listed in Table 1 (entry 7). Compared with entry 8 which provides 400 mg catalysts for 1 equiv. substrate, it should exhibit a similar theoretically collision probability between catalytic elements and substrate since only solvent is excessive for the test. Compared with entry 6 which provides 200 mg catalysts for 1 equiv. substrate, it has a relatively excessive amount of catalyst. Fig. S6 (Supporting information) shows the comparison of the conversions and yields among the three. It can be seen that the iodobenzene is transformed in 69.4% under IH and 61.9% under JH, which is close to entry 8 without further improvement. It further proves the conclusion above that the magnetic core presents higher surface temperature in excessive solvent. It is worth noting that the biphenyl yields of only 26.5% and 25.9% in both heating cases, which are far lower than the other two conditions. It may be attributed to the low concentration of the base, which limits the activation process of phenylboric acid and neutralization reaction of boric acid from cross-coupling [34].

Additionally, the experiment entries for different reaction time have been listed in Table S1 (Supporting information). Fig. S7 (Supporting information) shows the conversion of iodobenzene and yield of biphenyl, respectively, during the reaction at 54 °C by increasing the reaction time under the both cases. Interestingly, the IH scheme shows only a slight increase of iodobenzene conversions in the range of 63.5%–66.6% with prolonging the reaction time, compared with 49.4%–60.3% by using JH. And more than 7% difference between both cases on yield is also observed under the three reaction periods. A clear improvement in terms of the reaction rate is observed when operating the reaction under IH, evidenced by the higher iodobenzene conversion (63.5%) and biphenyl yield (49.4%) obtained in 1 h of reaction than those under JH within 3 h. Therefore, it can be confirmed that the reaction can reach the peak conversion with higher yield much more rapidly under IH than under JH. Such a result can be ascribed to the effectiveness of the IH approach, which supplies the heat for the catalyst directly and increases the localized temperature of the active sites at the same overall reaction media temperature. In fact, for many catalytic processes requiring heat to be supported, the limiting factor for the reaction rate is not the catalyst activity but the

Table 2
Suzuki-Miyaura cross-coupling results of other substrates in both cases using Fe_3O_4@C-Pd as catalyst.[a]

Entry	Aryl iodide	Arylboronic acid	Conversion (%)[b]	
			IH	JH
1	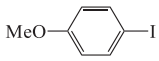	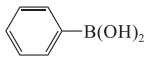	42.2	35.6
2	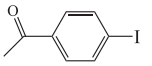	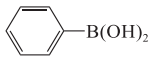	68.2	59.3
3	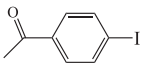	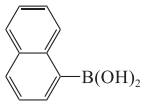	83.4	79.0

[a] Reaction conditions: arylboronic acid (1.5 equiv.), aryl iodide (1 equiv.), TBAB (2 equiv.), Na_2CO_3 (2 equiv.), H_2O (10 mL), catalyst (100 mg), reaction time (1 h), temperature (54 °C).
[b] Conversion of substrate and yield of biphenyl are determined by GC analysis.

heat transfer. Mortensen *et al.* [17,21] reported a series of dual-function Ni-Co catalysts with high-temperature characteristics for realizing steam methane reforming. They have also concluded that the induction-heated catalyst combining with the internal heating approach overcame the heat transfer from the heat source to the active sites, and would favor pushing the transformation process to the bounds of its intrinsic kinetics. Potentially, this unique approach enables catalytic transformation to utilize heat at a rate equivalent to the chemical reaction rate.

A control reaction without using any solid catalyst as a control (Table 1, entry 2) and a control reaction with only loading the naked Fe_3O_4 particles (Table 1, entry 4) were also conducted under JH at 54 °C as listed in Table 1. Minor performance (only 4.2% iodobenzene conversion and zero biphenyl yield) is found in the control reaction without using any solid (Table 1, entry 2). The same control test entry cannot be operated under IH as no inductive magnetic solid in the reaction media. While conversions of 19.1% under IH and 11.4% under JH are obtained for the control reactions conducted with using the naked Fe_3O_4 particles without Pd decoration (Table 1, entry 4). This suggests that the reaction performance is largely attributed to the catalytic activity of the Pd nanoparticles.

The experiments of using extended substrates for Suzuki-Miyaura cross-coupling reactions have been conducted, and the corresponding results are listed in Table 2. The substituted aryl iodide, such as 4-iodoanisole, 4-iodoacetophenone, and other arylboronic acid, such as 1-naphthylboronic acid, were used as substrates (Table 2, entries 1–3). The aryl iodide used in entry 1 (Table 2) contains an electron-rich group. Such substrates are relatively difficult to realize oxidative addition reaction, thus the catalytic performance is lower than that of unsubstituted iodobenzene as shown in Table 1. Conversely, the substrate in entries 2 and 3 (Table 2) provides electron-deficient groups due to formyl group, which are more prone to oxidative addition reaction. Similarly, the reactions supported by IH exhibit relatively high conversion of the substrates.

Fig. S8 and Table S2 (Supporting information) show the EDS mapping, SEM images and ICP-OES result of the used Fe_3O_4@C-Pd. It can be seen that the Pd content of the used catalyst in this study decreases obviously regardless of heating modes, evidenced by the ICP-OES result (Table S2) and EDS mapping images (Figs. S8a–c and e–g). This is mainly attributed to the lack of confinement on the active sites. We believe in the future work, a well materials design for encapsulating the Pd particles with an accessible solid layer is highly necessary, which will maximize the exposure of active sites and reduces the activity loss so as to increase the cyclic stability. Since the focus of the present study is to verify the effectiveness of IH in improving the catalytic performance compared with JH, thus the further functionalization of the microsphere catalyst in improving the stability has not been carried out.

In summary, efficient catalytic Suzuki-Miyaura cross-coupling reactions were achieved through novel IH manner enabled by using conductive superparamagnetic core-shell microsphere with supported Pd nanoparticles as catalysts. In the meantime, the same reaction sustained by JH has been conducted as a reference. Results show that, at the same apparent temperatures, the reactions supported by the IH all exhibit the better catalytic performance in terms of higher conversion and yield, when compared to the reactions sustained by conventional JH. The improvement is mainly attributed to the high efficiency of the heat transfer from the superparamagnetic core to the surface catalytic sites of microsphere catalyst. Moreover, it has be found that the reactions have been largely accelerated, resulting in much shorter reaction time required to approach a given value of reactant conversion. It has been demonstrated that such a unique heating method of IH combined with using superparamagnetic nanocatalysts is highly effective for supporting the heterogeneous liquid-solid catalytic reactions, which enables the reaction to achieve the same performance but maintain the reaction media at a much lower temperature. Specifically, for a given catalytic reaction which is sensitive to the temperature of the reactive sites, on the one hand, the heat generated directly around active sites within the catalyst particle makes the intrinsic reaction temperature uniform, thus reducing the by-products caused by high temperature gradient under conventional heating. On the other hand, such an IH method leads to relatively lower overall temperature of the reaction media, which can reduce energy input. Additionally, it can be envisaged that through precise nanocatalyst design, other inductive catalysts based on using either magnetic metals of Ni, Co or non-magnetic but conductive materials can also be developed, which will provide a largely expanded application scenarios for both liquid-solid and gas-solid heterogeneous reactions. We anticipate that the IH strategy with its unique outwards heat transfer properties, in the future, holds remarkable potential in achieving highly efficient industrial catalysis with improved energy efficiency, simplified reactor design and safety-enhanced operation.

Declaration of competing interest

The authors declare that they have no known competing financial interests or personal relationships that could have appeared to influence the work reported in this paper.

Acknowledgments

This work was supported by the National Natural Science Foundation of China (Nos. 52006032, 22001009) and the Natural Science Foundation of Anhui Province (No. 2008085QB60).

Supplementary materials

Supplementary material associated with this article can be found, in the online version, at doi:10.1016/j.cclet.2022.108101.

References

[1] G. Centi, S. Perathoner, Catal. Today 77 (2003) 287–297.
[2] R. Schlögl, Angew. Chem. Int. Ed. 54 (2015) 3465–3520.
[3] C. Duong-Viet, H. Ba, Z. El-Berrichi, et al., New J. Chem. 40 (2016) 4285–4299.
[4] Y.D. Wang, J. Shi, Z.H. Jin, et al., Chin. J. Catal. 39 (2018) 1147–1156.
[5] G. Xiong, J. Jia, L. Zhao, et al., Sci. Bull. 66 (2020) 386–406.
[6] S. Hamzehlouia, S.A. Jaffer, J. Chaouki, Sci. Rep. 8 (2018) 8940.
[7] M.B. Schütz, L. Xiao, T. Lehnen, et al., Int. Mater. Rev. 63 (2018) 341–374.
[8] H. Jiang, L. Tong, H. Liu, et al., Matter 2 (2020) 1535–1549.

[9] L. Li, J. Zhang, Z. Peng, et al., Adv. Mater. 28 (2016) 838–845.
[10] A. Bogaerts, G. Centi, Front. Energy Res. 8 (2020).
[11] N.A. Frey, S. Peng, K. Cheng, et al., Chem. Soc. Rev. 38 (2009) 2532–2542.
[12] S. Ruta, R. Chantrell, O. Hovorka, Sci. Rep. 5 (2015) 9090.
[13] X. Zhang, S. Chen, H.M. Wang, et al., Biomed. Eng. Appl. Basis Commun. 22 (2010) 393–399.
[14] S. Ceylan, L. Coutable, J. Wegner, et al., Chem. Eur. J. 17 (2011) 1884–1893.
[15] S. Ceylan, C. Friese, C. Lammel, et al., Angew. Chem. Int. Ed. 47 (2008) 8950–8953.
[16] J. Hartwig, S. Ceylan, L. Kupracz, et al., Angew. Chem. Int. Ed. 52 (2013) 9813–9817.
[17] P.M. Mortensen, J.S. Engbæk, S.B. Vendelbo, et al., Ind. Eng. Chem. Res. 56 (2017) 14006–14013.
[18] H.M. Nguyen, C.M. Phan, S. Liu, et al., Chem. Eng. J. 430 (2022) 132934.
[19] C. Scarfiello, M. Bellusci, L. Pilloni, et al., Int. J. Hydrog. Energy 46 (2021) 134–145.
[20] F. Varsano, M. Bellusci, A.L. Barbera, et al., Int. J. Hydrog. Energy 44 (2019) 21037–21044.
[21] M.G. Vinum, M.R. Almind, J.S. Engbaek, et al., Angew. Chem. Int. Ed. 57 (2018) 10569–10573.
[22] A. Meffre, B. Mehdaoui, V. Connord, et al., Nano Lett. 15 (2015) 3241–3248.
[23] A. Bordet, L.M. Lacroix, P.F. Fazzini, et al., Angew. Chem. Int. Ed. 55 (2016) 15894–15898.
[24] D. De Masi, J.M. Asensio, P.F. Fazzini, et al., Angew. Chem. Int. Ed. 59 (2020) 6187–6191.
[25] L. Truong-Phuoc, C. Duong-Viet, G. Tuci, et al., ACS Sustain. Chem. Eng. 10 (2021) 622–632.
[26] W. Wang, C. Duong-Viet, G. Tuci, et al., ChemSusChem 13 (2020) 5468–5479.
[27] W. Wang, C. Duong-Viet, Z. Xu, et al., Catal. Today 357 (2020) 214–220.
[28] J. Leclercq, F. Giraud, D. Bianchi, et al., Appl. Catal. B: Environ. 146 (2014) 131–137.
[29] T. Truong-Huu, C. Duong-Viet, H. Duong-The, et al., Appl. Catal. A: Gen. 620 (2021) 118171.
[30] J. Liu, Z. Sun, Y. Deng, et al., Angew. Chem. Int. Ed. 48 (2009) 5875–5879.
[31] Z. Sun, J. Yang, J. Wang, et al., J. Mater. Chem. A 2 (2014) 6071–6074.
[32] L. Botella, C. Nájera, J. Organomet. Chem. 663 (2002) 46–57.
[33] N. da Silva Moura, K.R. Bajgiran, A.T. Melvin, et al., ACS Appl. Nano Mater. 4 (2021) 13778–13787.
[34] M.J.S. Dewar, R. Jones, J. Am. Chem. Soc. 89 (1967) 2408–2410.